Synchronizing spiral waves in a coupled Rössler system

Gao Jia-Zhen(高加振), Yang Shu-Xin(杨舒心), Xie Ling-Ling(谢玲玲), and Gao Ji-Hua(高继华)†

Shenzhen Key Laboratory of Special Functional Materials, College of Materials, Shenzhen University, Shenzhen 518060, *China*

(Received 13 October 2010; revised manuscript received 10 November 2010)

The synchronisation of spiral patterns in a drive-response Rössler system is studied. The existence of three types of synchronisation is revealed by inspecting the coupling parameter space. Two transient stages of phase synchronisation and partial synchronisation are observed in a comparatively weak feedback coupling parameter regime, whilst complete synchronisation of spirals is found with strong negative couplings. Detailed observations of the synchronous process, such as oscillatory frequencies, parameters mismatches and amplitude variations, etc, are investigated via numerical simulations.

Keywords: synchronisation, spiral wave, coupled Rössler system

PACS: 05.45.–a, 82.40.Ck, 47.54.–r **DOI:** 10.1088/1674-1056/20/3/030505

1. Introduction

Spiral waves are interesting periodic patterns frequently observed in diverse spatiotemporal systems, such as chemical reactions, cardiac tissues, optical fields, physiological systems and hydrodynamics.[1−14] It has also been observed that spiral waves present complex behaviours and quasi-periodic oscillations.[15,16] Recently, the control of spirals in spatiotemporal systems has become a focused topic because of the fruitful application of pattern formations. Spiral waves are harmful and should be suppressed or removed in some cases, and the control of spiral waves is directly aiming at this goal. In this respect, the study of spiral stability is an important issue. The spiral pattern can be destroyed by near-core breakup, which can be interpreted as the Doppler effect,[17−19] and the far-field breakup, which is concerned with Eckhaus instability.[20,21] It is also revealed that a gradient force can induce spiral drift and deformation both theoretically and experimentally.[22−24] In addition, the synchronisation of extended systems has been an important research topic in recent decades because spatiotemporal systems are a rich reservoir of diverse phenomena and research of them is aimed at their practical application. It is well known that periodic signals can be injected into spatiotemporal systems; the chaotic motion can be suppressed and the system can be guided to the periodic orbits. In related publications, study is mainly focused on the stability of plane waves in one-dimensional or two-dimensional systems.[25−29] The research of coupled two-layer systems also reveals complex phenomena of pattern interaction in extended systems.[30−33] The controllability of injected signals with more complicated structures in high dimensional spatiotemporal systems should be an interesting topic and more closely related to realistic systems. To our knowledge, investigation of the stability of injected spiral waves in coupled systems is still at an early stage.[34−36] In this study, we take the coupled Rössler system and investigate the stability of injected spiral waves, and report new features within the synchronisation process.

2. Coupled Rössler system

In the polar coordinates system $(x, y) \rightarrow (r, \theta)$, spiral waves have the generalised form of $F(r)\exp\{\mathrm{i}[\sigma\theta - \omega t + \varphi(r)]\}$, where $F(r)$ and $\varphi(r)$ are real functions denoting the amplitude and phase of the system variables, and the integer σ is called the topological charge. Stable spiral waves can be found spontaneously in nature with $\sigma = \pm 1$, while stable target waves with $\sigma = 0$ can be sustained by local inhomogeneities or special boundary configurations.[37−39] Here, we consider the following Rössler oscillators with diffusive connections in an extended system[40,41],

$$\begin{aligned}\frac{\partial X}{\partial t} &= -Y - Z + d\nabla^2 X,\\ \frac{\partial Y}{\partial t} &= X + aY + d\nabla^2 Y,\\ \frac{\partial Z}{\partial t} &= b - Z(X - c) + d\nabla^2 Z,\end{aligned} \tag{1}$$

†Corresponding author. E-mail: jhgao@szu.edu.cn

© 2011 Chinese Physical Society and IOP Publishing Ltd

where X, Y, and Z are system variables; a, b, and c are system parameters, and d is the diffusive coefficient. In a 2D system, the Laplacian has the form $\nabla^2 = \dfrac{\partial^2}{\partial x^2} + \dfrac{\partial^2}{\partial y^2}$. System (1) can present various patterns with different combinations of system parameters and diffusive coefficients, such as spatiotemporal chaos and stable spiral waves, and has been extensively studied. Considering that Eq. (1) could present spiral motions, we inject the periodic signals into another Rössler oscillation system, therefore take Eq. (1) as a drive system, and the following response system has the form,

$$\begin{aligned}
\frac{\partial X'}{\partial t} &= -Y' - Z' + d'\nabla^2 X' + \varepsilon\,(X - X')\,,\\
\frac{\partial Y'}{\partial t} &= X' + a'Y' + d'\nabla^2 Y',\\
\frac{\partial Z'}{\partial t} &= b' - Z'\,(X' - c') + d'\nabla^2 Z',
\end{aligned} \tag{2}$$

where X', Y', and Z' are the system variables; a', b', and c' are system parameters, d' is the diffusive coefficient; ε is the negative feedback coupling strength. System (2) has a similar structure to system (1), and the system parameters and diffusive coefficient in system (2) can be different from those in system (1). In the following studies, drive system (1) is supposed as presenting spiral motions, and then the periodic signals can be transferred to response system (2) because of the existence of coupling interactions. Hereafter, we will take systems (1) and (2) as the drive-response model, and investigate the synchronisation of the spiral wave patterns by adjusting the system parameters and coupling strengths.

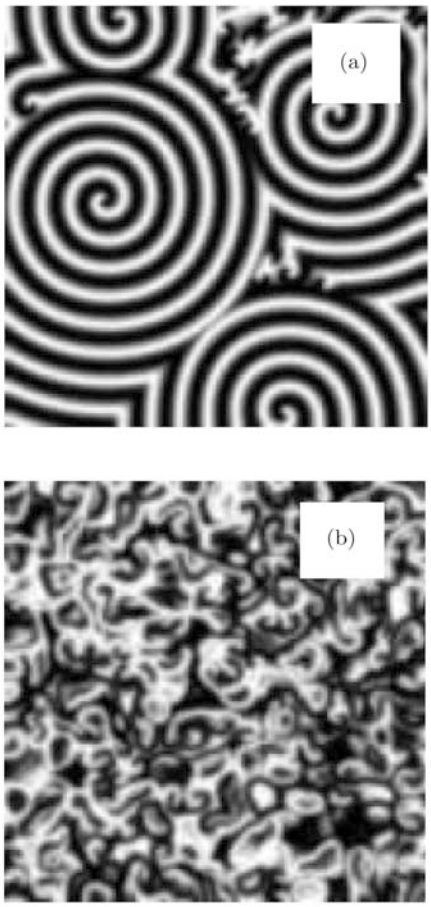


Fig. 1. Snapshots of variables X and X' for $\varepsilon = 0$. (a) Spiral wave with the system parameters $a = 0.2$, $b = 0.2$, $c = 2.5$, $d = 0.045$, (b) Spatiotemporal chaos with the system parameters $a' = 0.01$, $b' = 0.01$, $c' = 1.0$, $d' = 0.01$.

3. Numerical simulations

3.1. Synchronisation of patterns

First, we consider the situation of zero coupling $\varepsilon = 0$ a.u. (arbitrary units, in the following studies we use arbitrary units for all system and controlling parameters if there are no additional declarations), the original patterns of systems (1) and (2) can be different under nonidentical system parameters conditions. In Fig. 1, we plot examples of different spatiotemporal patterns in the $L \times L$ square area with no flux boundary conditions. In Fig. 1(a), multiple spiral waves in the area are found, and the boundaries of the spirals are clearly divided by hyperbolic lines. In Fig. 1(b), spatiotemporal chaos is presented when another set of system parameters are chosen for system (2). The disordered motion is distributed in the space and the orbit is chaotic everywhere.

Now we consider the spatiotemporal pattern synchronisation in Fig. 1 by injecting spiral signals from system (1) into system (2). We define the following functions to measure the average distances of every variable between the drive and response systems,

$$\sigma_X(t) = \frac{1}{L^2}\int_0^L \mathrm{d}y \int_0^L |X - X'|\mathrm{d}x, \tag{3a}$$

$$\sigma_Y(t) = \frac{1}{L^2}\int_0^L \mathrm{d}y \int_0^L |Y - Y'|\mathrm{d}x, \tag{3b}$$

$$\sigma_Z(t) = \frac{1}{L^2}\int_0^L \mathrm{d}y \int_0^L |Z - Z'|\mathrm{d}x. \tag{3c}$$

and the total error function of the drive–response systems is given by

$$\sigma = \lim_{T\to\infty} \frac{1}{T} \int_0^T [\sigma_X(t) + \sigma_Y(t) + \sigma_Z(t)]\, \mathrm{d}t. \quad (4)$$

Now we measure the difference between the drive system and the response system through the above index definitions. By inspecting the structures of $\sigma_X(t)$, $\sigma_Y(t)$ and $\sigma_Z(t)$, we learn that when $\sigma_X(t)$, $\sigma_Y(t)$, and $\sigma_Z(t)$ are near to zero, the differences of $X - X'$, $Y - Y'$, and $Z - Z'$ are comparatively small. Otherwise, the differences are large, and then the synchronisation between the drive and the response systems is not dominative. The definition σ in Eq. (4) is the total error function describing the global difference of the drive and response systems in a large time scale. In the following numerical experiments, we consider the small value of $\sigma \leq 0.1$ as the criterion for complete synchronisation, and this standard is applied throughout the paper without additional declaration. Then we study the synchronisation of coupled systems (1) and (2) by calculating the error functions in Eqs. (3) and (4). In Fig. 2(a), the initial pattern of response system (2) presents spatiotemporal turbulence. After

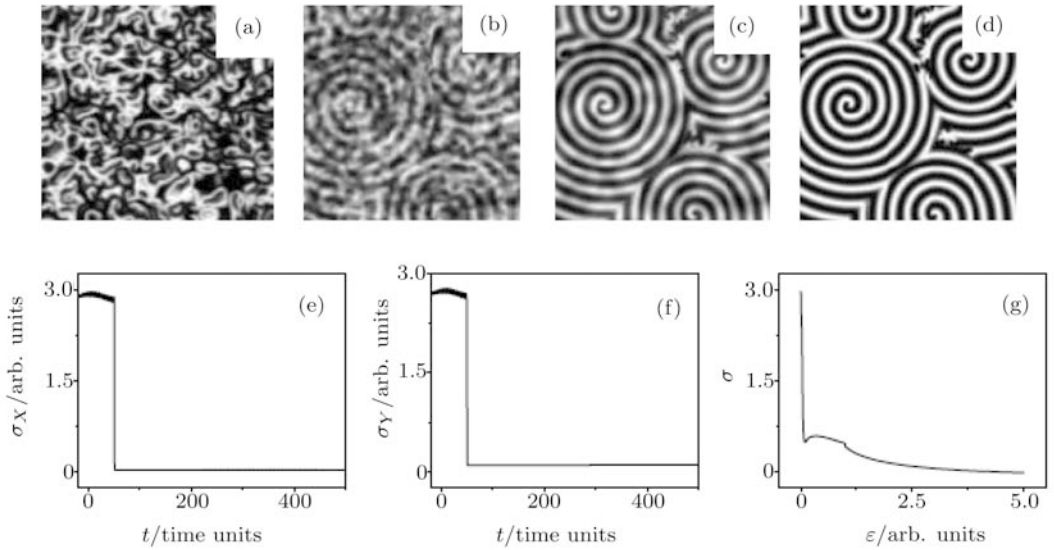


Fig. 2. The response system snapshots and the error functions. The system parameters of the drive and response systems are the same as those in Fig. 1. The coupling strength $\varepsilon = 0.2$. The snapshots of the variable X' in space at the system times (a) $t = 0$ t.u. (time units), (b) $t = 200$ t.u., (c) $t = 500$ t.u. and (d) $t = 3000$ t.u., respectively. (e) the error function $\sigma_X(t)$ versus time, (f) the error function $\sigma_Y(t)$ versus time, (g) the total error function σ versus coupling strength.

the coupling is switched on, with a comparatively large strength $\varepsilon = 0.2$ selected, the turbulent pattern of the response system is influenced by the injected spiral signals after the transient [Figs. 2(b) and 2(c)] and, finally, the response system achieves complete synchronisation with the drive system in Fig. 2(d). More precisely, we study this synchrous process by considering the error functions. In Figs. 2(e) and 2(f), the error functions are plotted versus system time. The originally large $\sigma_X(t)$ and $\sigma_Y(t)$ drop to near zero when the coupling is switched on, and these observations indicate a perfect synchronisation. Obviously, coupling strength plays an important role in the process. It is easy to predict that a large coupling intensity will lead to perfect synchronisation. In Fig. 2(g), the total error function σ is plotted versus coupling strength, and we observe that large ε corresponds to the small σ, and thereafter leads to a good synchronisation.

3.2. Phase space and frequency locking

To investigate the process of the above synchronisation in detail, we now compare the oscillatory trajectories in phase space and the frequency of the oscillation for the response system by varying coupling strengths. In Fig. 3(a), the variable X' is plotted versus system time, the chaotic trajectory is obvious when the coupling is off with $\varepsilon = 0$. In Fig. 3(b), the section of phase space ($X' - Y'$ plane) is plotted, and the non-periodic variable orbit confirms that

the oscillation is chaotic. In Fig. 3(c), the chaotic frequency distribution is indicated by the continuous spectrum in the case of zero coupling. Then the cases of finite couplings are considered in the following simulations. In Figs. 3(d), 3(e), and 3(f), the coupling strength is adjusted to $\varepsilon = 0.008$, the trajectories in phase space show the structure of a tori instead of chaotic motions, and two separated frequency peaks are observed. A new frequency, which is equal to the rotational frequency of the drive system, appears in the response system. Hereafter, when the coupling strength is increased to $\varepsilon = 0.0098$, we can observe that the new frequency peak grows and the old one shrinks in Figs. 3(g), 3(h) and 3(i). Finally, when the coupling strength is large enough, only the drive frequency dominates, and the response frequency is completely synchronous to the drive frequency.

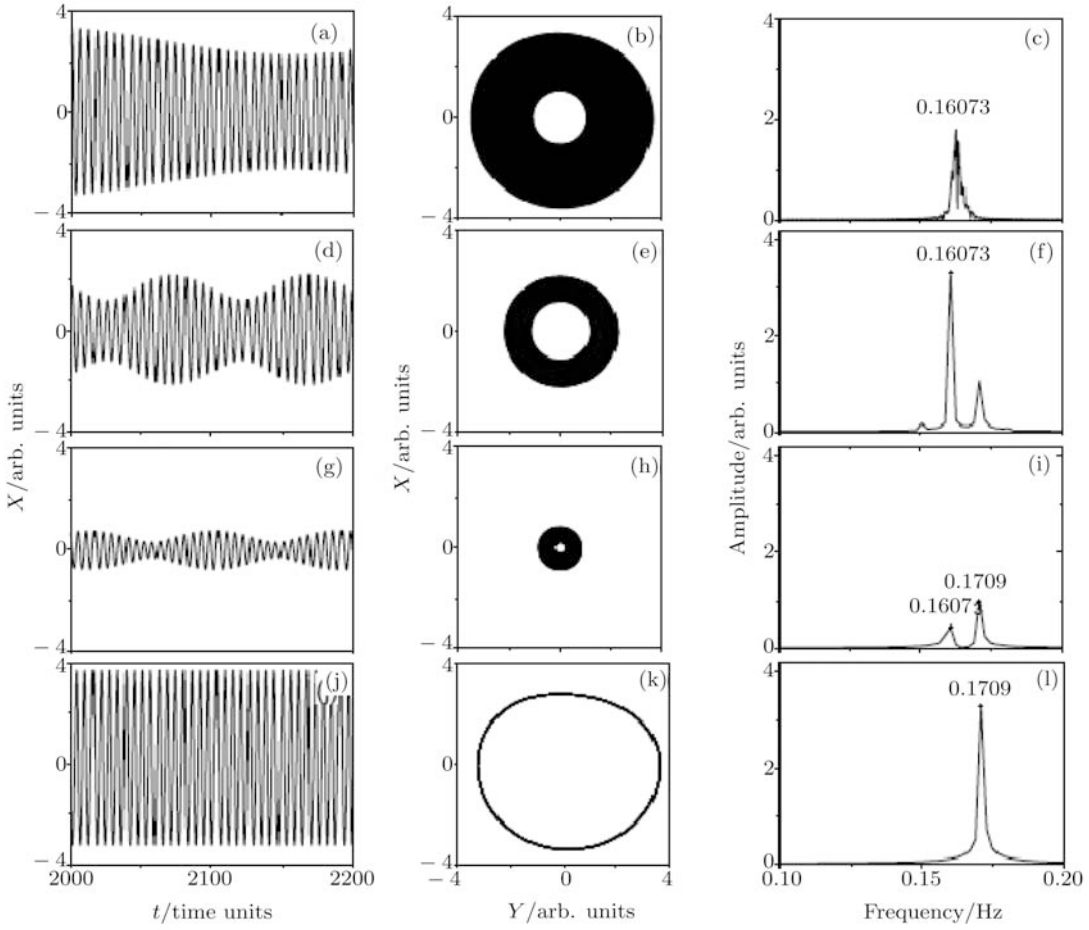


Fig. 3. The phase trajectories and the frequencies versus coupling strengths. (a) X' versus time, $\varepsilon = 0$, (b) $X' - Y'$ plane, $\varepsilon = 0$, (c) frequency distribution, $\varepsilon = 0$, the main peak is not obvious. (d) X' versus time, $\varepsilon = 0.008$, (e) $X' - Y'$ plane, $\varepsilon = 0.008$, (f) frequency distribution, $\varepsilon = 0.008$, there are two peaks, a new drive signal peak appears. (g) X' versus time, $\varepsilon = 0.0098$, (h) $X' - Y'$ plane, $\varepsilon = 0.0098$, (i) frequency distribution, $\varepsilon = 0.0098$, the old frequency peak shrinks and the new one dominates, (j) X' versus time, $\varepsilon = 0.2$, (k) $X' - Y'$ plane, $\varepsilon = 0.2$, (l) frequency distribution, $\varepsilon = 0.2$; the old frequency peak disappears completely, and the new frequency becomes the dominant one.

The transition from turbulent state to spiral motion in the response system is an interesting issue. It is notable here that synchronisation is achieved through a quasi-periodic route. In Fig. 3(c), the frequency spectrum of the variable trajectory is continuous, indicating a chaotic orbit. By increasing the coupling intensity in Fig. 3(g), we observe that a new frequency from the drive system emerges besides the original primary peak. The amplitude of the new frequency grows and becomes principal whilst the couplings increase. Phase synchronisation occurs in these observations. That is to say, the frequency of the drive system maps

into the response one, but the amplitude of system variables remains unlocked.

3.3. Amplitude variations

In the above section of phase space studies, we find that the variable amplitudes of the response system vary with coupling strength. In Figs. 3 (b), 3 (e), 3 (h), and 3 (k), the maximum and minimum ranges of the system vary during the transition from spatiotemporal chaos to spirals via the quasi-periodic route. To study these amplitude variations in detail, in Fig. 4(a), we plot the maximum and minimum amplitudes versus coupling strengths. Roughly,

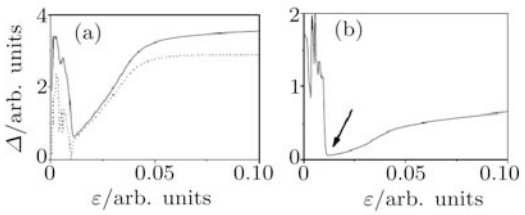


Fig. 4. The amplitude variations versus coupling strengths. (a) the maximum amplitude (solid line) and the minimum amplitude (dotted line), (b) the difference between the maximum and minimum amplitudes.

the amplitude changes can be divided into two types. In the first part of small coupling strength (for example, $\varepsilon < 0.02$), the response system is still in the chaotic state, and the amplitudes drop to near zero. With the increase of the coupling strength, the response system gradually becomes orderly. In the second part with comparatively large couplings, the amplitude variations increase with smooth curves, which are dramatically different from the former. For further contrast, Fig. 4 (b) is plotted to show the difference between the maximum and minimum amplitudes from chaotic oscillation to quasi-periodic motion. There is a coupling strength dividing the controlling parameter regime into two parts, and the variable difference is near to zero around this critical point [indicated by an arrow in Fig. 4(b)]. This is an interesting simulation result and we believe that further study of this critical phenomenon will spark new research directions.

3.4. Parameter mismatches

The controllability of synchronisation is influenced by many factors. One of the interesting things that concerns us is the impact of system parameters. As shown in Eqs. (1) and (2), the system parameter sets of the drive and response systems are (a, b, c, d) and (a', b', c', d'), respectively. In Fig. 5, we study the controllability by computing the global error flow, which is defined in Eq. (4), for different system parameters. In the cases of varying response system parameters, we observe that the error functions σ change with the parameter adjustment. With small system parameter mismatches, control is achieved with a small error function σ. We conclude that when the difference of the parameters between the drive system and the response system is larger, the drive–response synchronisation is more difficult; and when the difference is smaller, the synchronisation is easier.

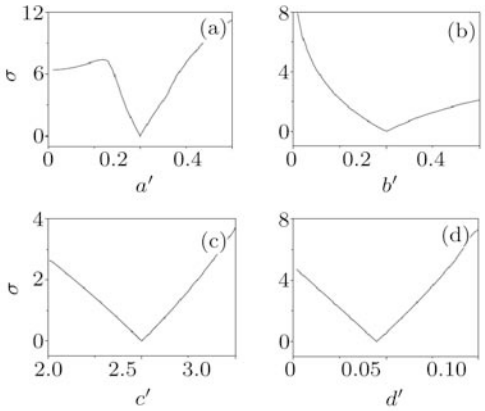


Fig. 5. σ versus system parameters. $a = 0.2$, $b = 0.2$, $c = 2.5$, $d = 0.045$, $\varepsilon = 0.05$, (a) σ versus a' for $b' = 0.2$, $c' = 2.5$ and $d' = 0.045$, (b) σ versus b' for $a' = 0.2$, $c' = 2.5$ and $d' = 0.045$, (c) σ versus c' for $a' = 0.2$, $b' = 0.2$ and $d' = 0.045$, (a) σ versus d' for $a' = 0.2$, $b' = 0.2$ and $c' = 2.5$.

3.5. Partial synchronisation

In the controlling process, we may observe the error functions to compare the difference between the three separated variables X, Y, and Z. In Fig. 6, we plot the error functions $\sigma_X(t)$, $\sigma_Y(t)$, and $\sigma_Z(t)$, which are defined in Eq. (3). When the control operation is switched on, the error functions drop down to near zero with a short transient, and this observation shows that the response system and the drive system reach synchronisation immediately at a strong coupling strength. Here, we set the same controllable criterion for error function ($\sigma \leq 0.1$) to imply perfect synchronisation. In Fig. 6, we find that when the control is switched on, the error functions $\sigma_X(t)$ and $\sigma_Y(t)$ are lower than 0.1 in a very short transient time, while $\sigma_Z(t)$ is more than 0.1 consistently. This can be considered as partial synchronisation. That is to say, the control can only synchronize partial variables [in this

case, the variables (X, X') and (Y, Y') are synchronized] and other variables [in this case, the variable (Z, Z')] remain asynchronous. This numerical observation reveals that the feasibility of synchronisation for three variables is different, and there is a partial synchronisation regime beyond the phase synchronisation observed in Section 3.2.

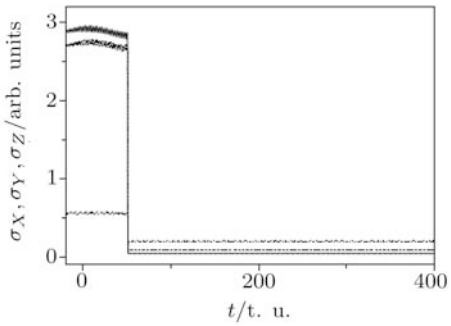


Fig. 6. The error functions $\sigma_X(t)$ (solid line), $\sigma_Y(t)$ (dashed line) and $\sigma_Z(t)$ (dotted line). $\varepsilon = 2.8$, other system parameters are the same as those in Fig. 1.

4. Conclusion

In conclusion, we have studied the synchronisation of spiral waves in the coupled Rössler system. Three types of synchronisation are found when the drive–response effect is considered, and many interesting features are presented by investigating oscillatory frequency locking, partial synchronisation and amplitude variations, etc. In the published works, the control and synchronisation of chaotic systems have been the focused topics in recent decades, and many techniques have been suggested and presented to suppress low and high dimensional chaotic systems. The control and synchronisation of periodic patterns, such as plane waves, spiral waves, target waves and scroll waves in spatiotemporal systems, are important tasks in the study of complex systems. Spiral waves have more complexity compared with the usual plane waves and are connected to the practical applications more closely. They emerge spontaneously in many realistic environments and can be considered as kinds of basic periodic and oscillatory cells in the natural world. In this research, we focus on spiral waves as the driving target and study the new features of the synchronisation. Three types of synchronisation are observed in the coupling system and many interesting phenomena are presented in detail. The phenomenology is intuitively believed to be ubiquitous in generalised drive–response systems when periodic spatiotemporal patterns are injected into the controlled system, and therefore has much importance in related research fields.

References

[1] Diercks J W and Anthes R A 1976 *J. Atmos. Sci.* **33** 959

[2] Winfree A T 1987 *When Time Breaks Down* (Cambridge: Princeton University Press)

[3] Yu L C, Ma J, Zhang G Y and Chen Y 2008 *Chin. Phys. Lett.* **25** 2706

[4] Jakubith S, Rotermund H H, Engel W, von Oertzen A and Ertl G 1990 *Phys. Rev. Lett.* **65** 3013

[5] Ecke R E, Mainieri R, Hu Y and Ahlers G 1995 *Science* **269** 1704

[6] Zhang H, Hu B and Hu G 2003 *Phys. Rev.* E **68** 026134

[7] Zhan M and Kapral R 2006 *Phys. Rev.* E **73** 026224

[8] Lee K J, Cox E C and Goldstein R E 1996 *Phys. Rev. Lett.* **76** 1174

[9] Xiao J H, Hu G and Hu B 2004 *Chin. Phys. Lett.* **21** 1224

[10] Zhan M, Luo J M and Gao J H 2007 *Phys. Rev.* E **75** 016214

[11] Gan Z N and Cheng X M 2010 *Chin. Phys.* B **19** 050514

[12] Xie L L and Gao J H 2010 *Chin. Phys.* B **19** 060516

[13] Zhong M and Tang G N 2010 *Acta Phys. Sin.* **59** 3070 (in Chinese)

[14] Deng M Y, Tang G N, Kong L J and Liu M R 2010 *Acta Phys. Sin.* **59** 2339 (in Chinese)

[15] Gong Y F and Christini D J 2003 *Phys. Rev. Lett.* **90** 088302

[16] Yuan G Y, Zhang G C, Wang G R and Chen S G 2005 *Commun. Theor. Phys.* **43** 459

[17] Bar M and Eiswirth M 1993 *Phys. Rev.* E **48** R1635

[18] Brusch L, Torcini A and Bar M 2003 *Phys. Rev. Lett.* **91** 108302

[19] Qian Y, Huang X D, Liao X H and Hu G 2010 *Chin. Phys.* B **19** 050513

[20] Ouyang Q and Flesselles J M 1996 *Nature* **379** 143

[21] Bar M and Or-Guil M 1999 *Phys. Rev. Lett.* **82** 1160

[22] Steinbock O, Schutze J and Muller S C 1992 *Phys. Rev. Lett.* **68** 248

[23] Gabbay M, Ott E and Guzdar P N 1999 *Phys. Rev.* E **59** 2443

[24] Zhang S L, Hu B and Zhang H 2003 *Phys. Rev.* E **67** 016214

[25] Hu G, Xiao J H, Gao J H, Li X M, Yao Y G and Hu B 2000 *Phys. Rev.* E **62** R3043

[26] Gao J H and Zheng Z G 2007 *Chin. Phys. Lett.* **24** 359

[27] Gao J H, Xie L L and Peng J H 2009 *Acta Phys. Sin.* **58** 5218 (in Chinese)

[28] Gao J H, Xie L L, Zou W and Zhan M 2009 *Phys. Rev.* E **79** 056214

[29] Qiu K, Tang J, Ma J and Luo J M 2010 *Chin. Phys.* B **19** 030508
[30] Hildebrand M, Cui J X, Mihaliuk E, Wang J C and Showalter K 2003 *Phys. Rev.* E **68** 026205
[31] Cui J X 2004 *Synchronisation of Spatiotemporal Patterns and Modeling Disease Speading Using Excitable Media* Ph. D. Dissertation (Morgantown: West Virginia University)
[32] Yang H J and Yang J Z 2007 *Phys. Rev.* E **76** 016206
[33] Rosenblum M G and Pikovsky A S 2001 *Phys. Rev.* E **64** 045202(R)
[34] Yang L F and Epstein I R 2003 *Phys. Rev. Lett.* **90** 178303
[35] Bragard J, Boccaletti S and Mancini H 2003 *Phys. Rev. Lett.* **91** 064103
[36] Bragard J, Boccaletti S, Mendoza C, Hentschel H G E and Mancini H 2004 *Phys. Rev.* E **70** 036219
[37] Jiang M X, Wang X N, Ouyang Q and Zhang H 2004 *Phys. Rev.* E **69** 056202
[38] Gao J H and Zhan M 2007 *Phys. Lett.* A **371** 96
[39] Eguiluz V, Hernandez-Garcia and Piro O 1999 *Int. J. Bifur. Chaos* **9** 2209
[40] Rössler O E 1976 *Phys. Lett.* A **57** 397
[41] Huang Z H and Dong Y L 2007 *Chin. Phys.* **16** 2291